Assessing indoor gas phase oxidation capacity through real-time measurements of HONO and NO x in Guangzhou, China

Jiangping Liu, Sheng Li, Jiafa Zeng, Majda Mekic, Zhujun Yu, Wentao Zhou, Gwendal Loisel, Adrien Gandolfo, Wei Song, Xinming Wang, et al.

Assessing indoor gas phase oxidation capacity through real-time measurements of HONO and NO_x in Guangzhou, China

Jiangping Liu,‡[ab] Sheng Li,‡[ab] Jiafa Zeng,‡[c] Majda Mekic,[ab] Zhujun Yu,[c] Wentao Zhou,[ab] Gwendal Loisel,[a] Adrien Gandolfo,[d] Wei Song,[a] Xinming Wang,[a] Zhen Zhou,[c] Hartmut Herrmann,[efg] Xue Li*[c] and Sasho Gligorovski *[a]

The hydroxyl radical (OH) is one of the most important oxidants controlling the oxidation capacity of the indoor atmosphere. One of the main OH sources indoors is the photolysis of nitrous acid (HONO). In this study, real-time measurements of HONO, nitrogen oxides (NO_x) and ozone (O_3) in an indoor environment in Guangzhou, China, were performed under two different conditions: (1) in the absence of any human activity and (2) in the presence of cooking. The maximum NO_x and HONO levels drastically increased from 15 and 4 ppb in the absence of human activity to 135 and 40 ppb during the cooking event, respectively. The photon flux was determined for the sunlit room, which has a closed south-east oriented window. The photon flux was used to estimate the photolysis rate constants of NO_2, $J(NO_2)$, and HONO, J(HONO), which span the range between 8×10^{-5} and 1.5×10^{-5} s^{-1} in the morning from 9:30 to 11:45, and 8.5×10^{-4} and 1.5×10^{-4} s^{-1} at noon, respectively. The OH concentrations calculated by photostationary state (PSS) approach, observed around noon, are very similar, *i.e.*, 2.4×10 and 3.1×10 cm^{-3} in the absence of human activity and during cooking, respectively. These results suggest that under "high NO_x" conditions (NO_x higher than a few ppb) and with direct sunlight in the room, the NO_x and HONO chemistry would be similar, independent of the geographic location of the indoor environment, which facilitates future modeling studies focused on indoor gas phase oxidation capacity.

[a]*State Key Laboratory of Organic Geochemistry, Guangzhou Institute of Geochemistry, Chinese Academy of Sciences, Guangzhou 510 640, China. E-mail: gligorovski@gig.ac.cn*

[b]*University of Chinese Academy of Sciences, Beijing 10069, China*

[c]*Institute of Mass Spectrometry and Atmospheric Environment, Jinan University, Guangzhou 510632, China. E-mail: tamylee@jnu.edu.cn*

[d]*Aix Marseille Univ., CNRS, LCE, UMR 7376, Marseille, 13331, France*

[e]*School of Environmental Science and Engineering, Shandong University, Qingdao, 266237, China*

[f]*School of Environmental Science and Engineering, Fudan University, Shanghai, 200433, China*

[g]*Leibniz-Institute for Tropospheric Research (TROPOS), Atmospheric Chemistry Department (ACD), Permoserstr. 15, 04318 Leipzig, Germany*

†Electronic supplementary information (ESI) available. See DOI: 10.1039/c9em00194h

‡ The first three authors contributed equally.

Introduction

A comprehensive understanding of oxidant levels and that of their precursors in indoor atmosphere is of great importance, considering their effects on the health of inhabitants. To understand the quality of air that we breathe on a daily basis, scientists have been intrigued by research on primary pollution sources and sinks in indoor environments.[1] Combustion processes (cooking, heating the residence, *etc.*) comprise one of the most important pollution sources in the indoor environment, especially in some Asian countries like China.[2,3] Nitrous acid (HONO) and nitrogen oxides (NO_x ¼ NO + NO_2) represent an important class of indoor pollutants emerging from combustion processes. The importance of

HONO arises from its well-known health impacts, *e.g.*, lowering of human lung functionality[4,5] and converting to different carcinogenic species, such as nitrosamines.[6–8] The importance of HONO has been further emphasized by observations of high HONO levels indoors[9–18] and its role as a precursor of the highly reactive hydroxyl radicals (OH) in the indoor air.[17] Nitrogen dioxide (NO_2) is a precursor of HONO through heterogeneous hydrolysis reactions and light- induced heterogeneous reactions occurring on various indoor surfaces.[19–26]

The contribution of HONO to the total OH budget in an indoor environment during the day was underestimated for a long time and has therefore been neglected in many models.[27,28] The first direct measurements of OH in indoor air[17] have shown that photolysis of HONO dominates the production of OH when the room is exposed to direct sunlight. Indeed, the UV fraction of sunlight can penetrate through windows and initiate the photochemical production of OH.[17,18,29–31] The effects of light emitted by indoor artificial lighting (LED, halogen lamps, fluorescent lamps) on potential photochemistry is still under discussion,[32,33] although it has been shown that renox- ification can occur on paint surfaces upon irradiation with indoor lighting.[34] Emission of HONO is much more pronounced when the indoor walls painted by photocatalytic paints are irradiated by direct sunlight in the presence of NO_2.[25,26] Knowl- edge about the formation of OH on an hour-to-hour and season- to-season basis at different geographic locations is of paramount importance to developing more accurate models[35] describing the secondary chemistry in the indoor environment.[3,28,36–42]

Indoor HONO was first identified and measured by James Pitts and coworkers using differential optical absorption spec- troscopy (DOAS).[43] Since then, several studies have attempted to measure indoor HONO levels by indirect techniques (denuders, passive samplers, *etc.*).[14,15,18,44] However, measuring NO_x and HONO at the same time represents an experimental challenge due to the possible sampling artefacts and chemical interfer- ence during the measurements.[45,46]

For example, observations by Spicer *et al.* (2001)[47] demonstrated that nitrous acid represents a quantitative interference to NO_2 measurements by three different passive sampling techniques. In this study, real-time measurements of NO, NO_2, HONO, and O_3 were performed in an indoor environment to better characterize their mixing ratios, sour- ces, and sinks under two different scenarios: (1) in the absence of any human activity and (2) in the presence of cooking. This study is the first campaign in China and worldwide employing the long path absorption photometer (LOPAP) for real-time measurements of HONO[48,49] in an indoor environment. We also measure spectral irradiance from sunlight penetrating through the windows into the room and determine the photolysis rates of HONO and NO_2 under different conditions. The photolysis rates of HONO and measured mixing ratios of NO, NO_2 and HONO are used to estimate OH concentrations by pseudo stationary state (PSS) approach and to compare the estimated OH concentrations under different conditions.

Methods summary

The experimental campaign was performed in the period 01–15 December in a lab room of the following dimensions: 3.7 m (length) × 2.2 m (width) × 2.8 m (height), situated at Jinan University, Guangzhou, China (Fig. S1†). There was one window with dimensions 1.1 m × 0.9 m. The lab room was oriented south-east. CO_2 was added as dilution tracer through the main door before the background experiments in order to measure the air exchange rates. During the cooking scenario, the decay of CO_2 released by the gas stove was monitored to estimate the air exchange rate. Two fans were installed in the corners to ensure air homogeneity in the lab room. Each set of measurements (in the absence of human activity and in the presence of cooking) during different periods of the day was repeated at least twice. The combustion appliance consists of a natural gas stove. Peanut oil was used for the cooking experiments. The cooking experiments lasted about 15 to 20 min. The cooking scenario in this lab room can be compared with cooking in a typical residence without using a fume hood.

All the instruments were placed in the neighbouring room (Fig. S1†). NO_x, O_3 and CO_2 were sampled by Teflon tubes with *ca.* 2 m length going through a hole made in the wall to the lab room at 2 m distance from the gas stove and 1 m from the flat collector of the spectroradiometer. For HONO measurements, the sampling port was placed directly in the lab room nearby the flat collector of the spectroradiometer and at 2 m distance from the gas stove. To prevent clogging of the instrument, a cyclone aerosol size selector was installed prior to the sampling port to remove the coarse particles. A Teflon tube about 40 cm long was connected between the cyclone aerosol size selector and the sampling port.

It has to be noted that the VOC composition and mixing ratios of the oxidants (NO_x, O_3) depend on both indoor and outdoor sources. The OH concentration depends strongly on the actinic flux and, hence, the orientation of the room, the solar zenith angle, and the thickness and nature of the windows glass.[29] Therefore, the values of the measured NO_x, O_3 and HONO mixing ratios correspond to this particular indoor environment.

Real-time instruments

Online instruments were used for time-resolved measurements of HONO, NO, NO_2, O_3, VOCs, carbon dioxide (CO_2), relative humidity (RH), and temperature (*T*). For HONO measurements, LOPAP (QUMA, Germany), was used, for which the operational procedure is described in detail elsewhere.[48,49] Briefly, HONO is sampled in a stripping coil by a fast chemical reaction and converted into an azo dye, which is photometrically detected by long path absorption in a special Teflon tubing (Teflon AF2400).

During all the experiments, the detection limit was smaller than 30 parts per trillion (ppt), with a total accuracy of ±10% and measured time response of about 5 min under the operation conditions applied (gas flow and pump flow of 1 l min^{-1} and 500 ml min^{-1}, respectively).

The mixing ratios of NO_x, NO_2 and NO were simultaneously measured by a chemiluminescence instrument (CLD 88p, Eco Physics, Switzerland) coupled to a photolytic (metal halide lamp) converter (PLC 860, Eco Physics, Switzerland). The NO_x analyzer is very sensitive, with a detection limit of 110 ppt. The photolytic converters have about 10% interference against HONO.[50] Conservatively, it is suggested that a positive bias of up to 1 ppb in the accuracy of the measurements may have been possible, which falls in the range of the stated 10% uncertainty.

The mixing ratios of O_3 were measured by calibrated ozone analyzer (Thermo Scienti□c Model 49i, USA). The detection limit of this O_3 analyzer is 0.5 ppb, with a time resolution of 20 s. The CO_2 decay was monitored online by time-of-□ight single-photon ionization mass spectrometry, (TOF-SPIMS; SPIMS 3000, Hexin Analytical Instrument Co., Ltd., China) with a time resolution of one second. Polydimethylsiloxane (PDMS, thickness 0.002 int, Technical Products Inc, USA) membrane was used in the injector of the TOF-MS. A vacuum ultraviolet (VUV) light generated by a commercial D2 lamp (Hamamatsu, Japan) was used for ionization of the molecules. Single-photon ionization, with 10.8 eV energy of the single photon, is capable of performing the "so□" ionization of the detected organic compound.

The ToF mass analyzer consists of a double pulsed acceleration region, a □eld-free dri□ tube, a re□ector and an ion detector. This TOF-MS has a LOD of approximately 1 ppb for most of the trace gases.[51] The average air exchange rate calculated from the decay of CO_2 was *ca.* 0.6 h^{-1}, in agreement with previous studies focused on observations in residences.[18,52–54] For example, the air exchange rate during a □ve-day period in a residence situated in Toronto, Canada, varied in a range between 0.19 and 0.74 h^{-1}, with an average value of 0.5 h^{-1}.[53] Zhou *et al.* (2019)[54] estimated a mean air exchange rate of 0.69 (±0.30) h^{-1} during cooking events in an occupied home at Syracuse, New York.

Results and discussion

Spectral irradiance and photolysis rates of NO_2 and HONO

The variation of sunlight intensity during the day, at diff erent latitudes and seasons, is an important parameter because it can alter the chemistry of various indoor environments. This is due to the fact that photochemistry plays an important role in the formation of free radicals such as OH.[29–31,36] The spectral irra- diance was measured during diff erent periods of the day (Fig. 1). Photon □uxes were estimated from spectral irradiance following a conversion procedure described elsewhere to calculate *J* values of HONO and NO_2.[17] Certainly, the conversion procedure will aff ect the calculations of *J* values of HONO and NO_2, performed therea□er. The variation of the determined actinic □ux during the direct irradiation of the room in the period between 9:30 a.m. and 12:15 p.m. on December 3rd is shown in Fig. 1. For comparison, the spectral actinic □uxes calculated with the tropospheric ultraviolet and visible (TUV) model (TUV version 5.3)[55] are also shown for outdoors with cloudless conditions at 12:15 p.m. on December 3rd.

Fig. 1 shows that the closed glass window □lters out the wavelengths below 330 nm, but still, an important fraction of

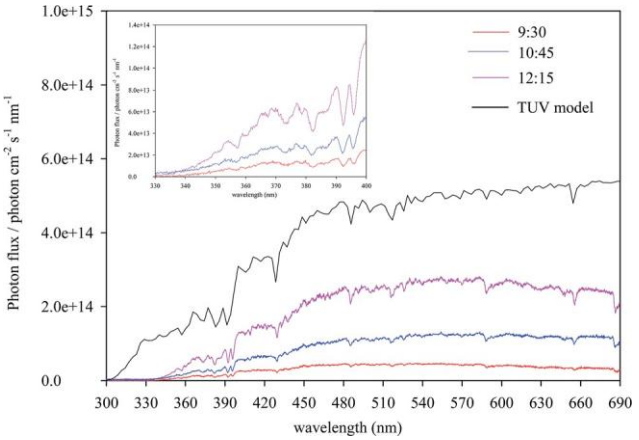

Fig. 1 Comparison of indoor actinic fluxes measured in direct sunlight in the lab room with the outdoor solar actinic flux determined by the TUV model. The TUV actinic flux is determined for Guangzhou (latitude 23.12899, longitude 113.12899), solar zenith angle (SZA) of 56.10° on December 3rd, at 12:15 p.m. The inset shows the indoor actinic fluxes in the UV range (330 nm < **l** < 400 nm).

UV light (330 nm # l # 400 nm) penetrates indoors, which can allow the photochemistry to occur. The determined actinic □ux from the sunlight penetrating indoors was used to calculate the □rst-order photolysis rate constants of HONO, *J*(HONO), and NO_2, *J*(NO_2).[56]

$$J = \sum_{\lambda=330\text{nm}}^{\lambda=\lambda_i} F(\lambda)\sigma(\lambda)\varphi(\lambda)\Delta\lambda \quad (1)$$

where *F* is the actinic □ux summed over the wavelength interval D**l** (photons cm^{-2} s^{-1}), *J* is the photolysis rate constant (s^{-1}), s(l) (cm^2) is the absorption cross-section, and f(l) (dimensionless) is the photolysis quantum yield of either NO_2 or HONO.

The sum in eqn (1) is performed from the lower limit of wavelengths available in this indoor environment, l = 330 nm, to a certain wavelength l_i at which either the primary quantum yield or the absorption cross section of either HONO or NO_2 becomes negligible. The recommended values of the quantum yields for NO_2 photolysis and absorption cross sections were used for the calculations of *J*(NO_2).[57]

Indeed, HONO photolysis occurs at wavelengths 300 nm # l # 405 nm.[58] As the wavelengths between 330 and 405 nm are readily transmitted indoors,[17,18,29–31] the HONO photolysis produces OH radicals as follows:

$$\text{HONO} + h\nu \rightarrow \text{OH} + \text{NO} \quad (\text{R1})$$

The recommended absorption cross sections for the *J*(HONO) calculations were used.[57] Measuring the quantum yields for R1 represents an experimental challenge because of contamination of the HONO by other strongly absorbing species, like NO_2, requiring corrections for their contributions to the absorption.[56] It is usually assumed, for a maximum photolysis, that the quantum yield for R1 is 1 at **l** < 400 nm.[59]

The photolysis rate constants of NO_2 and HONO calculated from the measured spectral irradiance in direct sunlight in the lab room are shown in Fig. 2.

The asymmetric time-dependence of J(HONO) and $J(NO_2)$ values can be partly explained by the change in the incidence angle of the sunlight and the reflection of sunlight from indoor surfaces after 12:00 leading to higher light transmission. Indeed, the higher SZA leads to increased intensity of re□ected light from the indoor walls.[29] In the morning, between 9:30 and 11:45, the room was irradiated with sunlight intensity that yields an average J(HONO) of 1.5×10^{-5} s^{-1} and $J(NO_2)$ of 8×10^{-5} s^{-1}. However, at noon, the J(HONO) and $J(NO_2)$ values peaked at 1.5×10^{-4} s^{-1} and 8.5×10^{-4} s^{-1}, respectively. These values are in excellent agreement with the peak values of J(HONO) ¼ 1.5×10^{-4} s^{-1} and $J(NO_2)$ ¼ 8×10^{-4} s^{-1} recorded on 21/07/2011 in a classroom in Marseille, France,[17] although the classroom was exposed to direct sunlight in the evening (17:00–19:00), and also in agreement with J(HONO) ¼ 7.2×10^{-5} s^{-1} and $J(NO_2)$ ¼ 8.5×10^{-4} s^{-1} determined for a sunlit region (around noon) in a residence in New York.[18] Gandolfo *et al.* (2016)[29] used a 2p spectral radiometer to measure the spectrally resolved actinic □ux in a room situated in Marseille, France, during summer and winter periods. These authors measured a maximum J(HONO) ¼ 1.7×10^{-4} s^{-1} during the summer period and J(HONO) ¼ 1.4×10^{-4} s^{-1} during the wintertime, in a sunlit room. The maximum value observed for $J(NO_2)$ in direct sunlight was 1.4×10^{-3} s^{-1} during summertime and 1.2×10^{-3} s^{-1} during wintertime. Both the J(HONO) and $J(NO_2)$ values measured during the winter and summer period are very similar with the corresponding values in this study, demonstrating that in sunlit regions of the room, the photolysis rate constants of HONO and NO_2 exhibit similar values independent of the season and geographic location. This is an important outcome of this study with respect to future modelling studies of indoor air photochemistry, in particular, regarding the modelling of OH radical chemistry.

These J(HONO) and $J(NO_2)$ values are smaller compared to the outdoor photolysis rate constants of HONO and NO_2 (*e.g.*, near the closed window, with up to 50% of outdoor sunlight[29]). For example, the mean values of J(HONO) and $J(NO_2)$ determined for the day period between 12:00 and 16:00 during the summer in a rural site of Guangzhou were 1.2×10^{-3} and 6.6×10^{-3} s^{-1}, respectively.[60] The peak values of J(HONO) and $J(NO_2)$ during that same campaign were 1.8×10^{-3} and 1×10^{-2} s^{-1}. A similar peak value of J(HONO) ¼ 1.6×10^{-3} s^{-1} was observed during the Berlioz campaign near Berlin, Germany.[61] Peak values of $J(NO_2)$ reached 1×10^{-2} and 8×10^{-3} s^{-1} during the field campaigns in Santiago de Chile, Chile,[62] and Thessaloniki, Greece,[63] respectively. Although the maximum indoor values of J(HONO) and $J(NO_2)$ are smaller in comparison to the corresponding outdoor values, they induce photochemical reactions and OH production in the sunlit indoor environment (*vide infra*).

In the afternoon, between 14:00 and 15:00, the mean J(HONO) and $J(NO_2)$ again dropped to 1.9×10^{-5} and to 1×10^{-4} s^{-1}, respectively, as was the case in the morning—indicating that photochemistry can be operational during the long period of the day (from 9:00 to 15:00) in this particular indoor environment.

HONO, NO_x and O_3 mixing ratios in the absence of human activity and during the cooking event

During the cooking event, peaks of HONO and NO_2 of about 40 ppb and 133 ppb were detected, respectively (Fig. 3).

The observed HONO values during the cooking activity are much higher compared to previous studies that used passive samplers, which have very poor time resolution (days to weeks) and cannot detect the huge variations that occur due to the combustion process. For example, Leaderer *et al.*[64] reported HONO levels of about 5 ppb, observed during the winter in houses with gas ranges in Albuquerque, New Mexico. The average indoor HONO concentration measured by passive sampler was 4.6 ppb in the presence of a gas range in Southern California homes.[14]

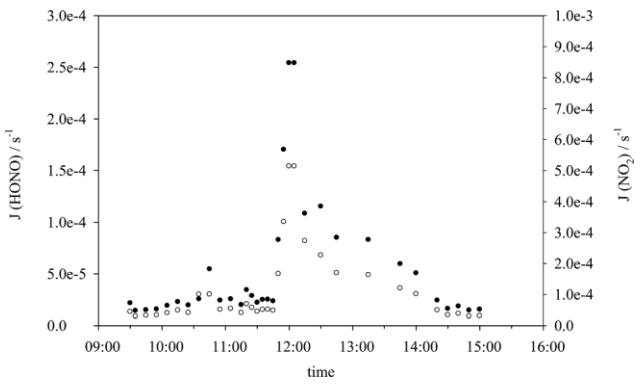

Fig. 2 The photolysis rate constants of HONO (**B**) and NO_2 (**C**) in the period between 9:30 a.m. and 3 p.m. on December 3rd, in the lab room in Guangzhou.

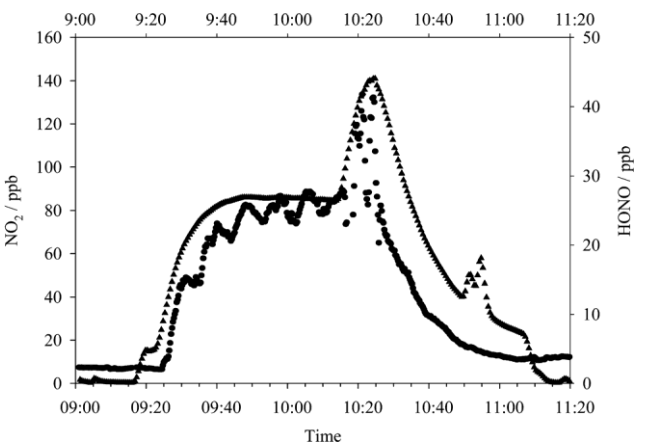

Fig. 3 The mixing ratios of (**:**) HONO and (**C**) NO_2 during a cooking event at December 07 2018 in the lab room on the campus at JNU, Guangzhou, China. The combustion started with ½ flame at 9:17. At 10:20, the knob of the gas appliance was turned to the maximum. The sharp increase of both NO_2 and HONO mixing ratios at 10 : 20 correspond to the increased combustion regime (maximum gas flame) of the gas appliance.

The average HONO mixing ratio during daytime and in the absence of any human activity was in the range between 3 and 4 ppb (see, *e.g.*, Fig. S3†). This value agrees with the HONO levels measured at similar indoor conditions. Recently, Zhou *et al.* (2018)[18] reported an indoor background HONO mixing ratio of 4.0 ± 2.5 ppb in an occupied home at Syracuse, New York. Average HONO levels of about 5 ppb were also detected in a classroom in Marseille at ambient conditions when extra NO_2 was not added in the classroom.[17] A mean HONO value of 5.3 ppb was observed in a residence situated in Toronto, Canada.[53] Collins *et al.* (2018)[53] have shown that indoor surfaces play an important role as a source and sink of HONO, impacting its balance. Indeed, NO_2 is a precursor of HONO through dark and light-induced heterogeneous reactions with indoor surfaces.[19,20,22–25,65] In this study, the average background NO_2 mixing ratio in the lab room in Guangzhou was 12.4 ppb (Fig. S3†), which is higher than the background NO_2 mixing ratio (2 ppb) measured at the house in Syracuse, New York[18] and lower than the mean background NO_2 level (30 ppb) measured in the classroom in Marseille.[17] In the absence of *in situ* sources, the indoor NO_2 level strongly depends on the outdoor NO_2, which can infiltrate indoors through the ventilation. For example, the lab room is located in a building at the campus of JNU far away from the main road, while the classroom in Marseille was located in a building on the main road with frequent vehicular traffic. During the cooking event, the NO_2 mixing ratio greatly increased, peaking at 133 ppb (Fig. 3), which is much higher than the previously reported NO_2 values in the presence of cooking (30 ppb)[54] and other combustion sources (17.3 ppb,[18] 52 ppb[14]). To our best knowledge, the reason for the small fluctuations of NO_2 in the period between 9:40 and 10:20 is not known (Fig. 3). The NO mixing ratios during the cooking activity rose to 180 ppb, while Zhou *et al.*[18] reported a NO peak of about 113 ppb during the cooking. However, Zhou *et al.* (2019)[54] reported a NO peak value of about 180 ppb during the cooking event in a residence near New York.

The ratio between HONO and NO_2 is an important indicator of the heterogeneous NO_2 / HONO conversion on indoor surfaces.[14,19–22] In this study, the average HONO/NO_2 background scenario is 0.36, which is higher than the HONO/NO_2 ratio of 0.17 and 0.08 measured in Californian homes and in Albuquerque residences, respectively.[12,14] This value of 0.36 is also higher than the HONO/NO_2 ratio of 0.13, which was recently observed in a residence in Toronto at RH (36–40%).[53] A very high mean ratio of 1.4 averaged over both events (background scenario and cooking) was recently observed in a residence in New York, indicating that HONO represents a significant fraction of the oxidized nitrogen burden in that residence.[18] When oxidant concentrations decreased to background conditions, the HONO/NO_2 ratio doubled to 2.2, indicating secondary chemical sources of HONO in that particular residence in New York.[18] Previous studies reported HONO/NO_2 ratios in the range between 0.1 and 0.3 (ref. 14–16 and 64) in residences with electric ranges, gas ranges and gas stoves. During the cooking event, we did not consider the HONO/NO_2 ratio, as HONO and NO_2 are directly emitted by the combustion process; hence, total HONO cannot be entirely considered as a product formed during the heterogeneous reaction of NO_2 with indoor surfaces.

The mixing ratios of another important indoor oxidant, ozone (O_3),[66] were at sub-ppb levels in the duration of the campaign except the ventilation periods, when O_3 was penetrating indoors from outside. Under the conditions considered in this study, O_3 does not play a role as an oxidant; hence, NO_2, HONO, and OH are the key players in this particular indoor environment. This is also in agreement with some very recent measurements of O_3 mixing ratios in residences in North America.[18,53] O_3 mixing ratios were less than 10 ppb in a residence in Toronto, which was lower than or similar to outdoor O_3 values. In a residence in New York, the O_3 mixing ratios were at sub-ppb levels for the entire campaign except during periods of significant infiltration of outdoor air. These measurements indicate that O_3 is a less important oxidant indoors than previously thought. Arguably, O_3 could be adsorbed on various indoor surfaces and play a role in heterogeneous reactions;[41,66] however, its presence in the gas phase was negligible during the recent measurements in residences in North America[18,53] and in this study. Future O_3 measurements in different dwellings are necessary to confirm or disprove this hypothesis.

Pseudo photostationary state (PSS) model

The pseudo photostationary state (PSS) model can be used to estimate the OH concentrations at NO_x levels higher than a few hundred ppts.[17,62,67] Since, in this study, the measured NO_x levels in both scenarios (in the absence and presence of cooking) were in the order of tens of ppbs, the secondary OH production can be balanced with the secondary OH loss.[17,62,67–71] In other words, the RO_2 and HO_2 initiators should not be considered as net OH sources because the consumption of OH through the reactions with VOCs (OH + VOCs) is balanced by the OH produced through HO_2 recycling (HO_2 + NO) without a significant additional secondary OH production. As a result of the balance between secondary OH production and elimination, the total rates of OH initiation and loss can be estimated by considering only the net OH sources and sinks implemented in the PSS model (*vide infra* eqn (4)). The excellent agreement between the OH concentrations modelled by comprehensive master chemical mechanism (MCM) and PSS approach during both seasons, winter and summer, in Santiago de Chile[67] confirms that the PSS model can reasonably explain the OH concentrations in an indoor environment with high NO_x levels. Hence, the PSS approach seems to be an appropriate tool to model the OH concentrations in the lab room under the experimental conditions in this study. Performing a detailed master chemical mechanism (MCM) model[72] is beyond the scope of this study, but it is recommended for future studies. In the PSS model, the primary OH sources are balanced with the OH sinks, $P_{OH}(\text{prim}) = P_{OH}(\text{loss})$. The primary OH production rate $P_{OH}(\text{prim})$ is given as follows:

$$P_{OH}(prim) = J(HONO)[HONO] + J(O^1D)[O_3]F_{OH} + \sum k_{O_3+alkene}[alkene][O_3]F_{OH_2}, \quad (2)$$

where J(HONO) (s^{-1}) is the photolysis first-order rate constant of HONO, [HONO] (molecules per cm^3) is the concentration of HONO, $J(O^1D)$ (s^{-1}) is the photochemical formation rate constant of $O(^1D)$ from O_3 photolysis, [O_3] is the ozone concentration (molecules per cm^3), F_{OH} is the yield of OH formation due to photolysis of ozone, $k_{O_3+alkene}$ (cm^3 per molecule per s) is the rate constant for the reaction between O_3 and the corresponding alkene, and F_{OH_2} is the yield of OH formation due to ozonolysis of alkenes. The loss rate of OH can be presented as follows:

$$P_{OH}(loss) = k_{OH+NO}[OH][NO] + k_{OH+NO_2}[OH][NO_2] + k_{OH+HONO}[OH][HONO]/molecules\ per\ cm^3\ per\ s, \quad (3)$$

where k_{OH+NO}, k_{OH+NO_2}, and $k_{OH+HONO}$ (cm^3 per molecule per s) are the rate constants for the reactions between OH and NO, OH and NO_2, and OH and HONO, respectively. Eqn (3) is valid under the assumption that the radical propagation by VOC oxidation is sufficiently fast (L(OH)VOCs = P(OH)VOCs).[62,67]

As a result, OH_{PSS} can be estimated with the following equation:

$$OH_{PSS} = \frac{J(HONO)[HONO] + J(O^1D)[O_3]F_{OH_1} + \sum k_{O_3+alkene}[alkene][O_3]F_{OH_2}}{k_{OH+NO}[NO] + k_{OH+NO_2}[NO_2] + k_{OH+HONO}[HONO]} \quad (4)$$

The $J(O^1D)$ due to ozone photolysis can be neglected, as the UV fraction of sunlight ($\lambda < 320$ nm), which is responsible for the photodissociation of ozone, is filtered out by the glass window (Fig. 1). The photon flux emitted from the artificial light available in the lab room is also not sufficient to photolyse ozone (Fig. S1†), in agreement with Kowal *et al.*, 2018.[31] As the concentrations of ozone were also very low, at sub-ppb levels, the second and third term in eqn (4) can be neglected.

Finally, the PSS model described in eqn (4) becomes:

$$OH_{PSS} = \frac{J(HONO)[HONO]}{k_{OH+NO}[NO] + k_{OH+NO_2}[NO_2] + k_{OH+HONO}[HONO]} \quad (5)$$

In this study, we applied eqn (5) to calculate the OH concentrations in the absence of human activity and during a cooking period. The obtained OH_{PSS} concentrations under both case scenarios are shown in Fig. 4.

The average daytime OH_{PSS} value at background scenario is 3.7×10^5 cm^{-3}. Very similar averaged daytime values were obtained during the cooking activities *i.e.*, $OH_{PSS} = 3.1 \times 10^5$ cm^{-3} and 3.8×10^5 cm^{-3} for the cooking periods in the morning (10:15–10:30 and 11:45–12:00, respectively). However, high OH_{PSS} concentrations were observed around noon, spanning the range between 1.4×10^6 cm^{-3} and 3.1×10^6 cm^{-3} during the cooking events and 2.4×10^6 cm^{-3} in the background scenario, which are in excellent agreement with the directly measured peak OH concentrations of *ca.* 2×10^6 cm^{-3} in a classroom in Marseille, France.[17] The cooking events carried out in the morning and noon periods only slightly influenced the peak OH concentrations compared to the background scenario. The most important parameter is the spectral irradiance of the sunlight that is transmitted through the windows. The peak OH concentrations formed through photolysis of HONO would largely depend on the spectral irradiance, the thickness of the glass windows, the solar zenith angle and the orientation of the room.[29]

There is excellent agreement between the maximum indoor OH_{PSS} concentrations in Guangzhou of 3.1×10^6 cm^{-3} and the OH_{PSS} concentrations determined in the classroom in Marseille of 1.8×10^6 cm^{-3} (ref. 17) due to the similar OH production rates. Indeed, for the background scenario (without human activity), the maximum OH production rate from this study of 2.5×10^7 radicals cm^{-3} s^{-1} is similar to the maximum OH production rate of 2.9×10^7 radicals cm^{-3} s^{-1} due to HONO photolysis, although the classroom in Marseille was northwest oriented, allowing direct sunlight in the room only in the evening (17:00–19:00).[17] The maximum OH production rate from this study of 2.5×10^7 radicals cm^{-3} s^{-1} for the background scenario is 3 times higher than the OH production rate of 8.3×10^6 radicals cm^{-3} s^{-1} calculated in the sunlit area of an occupied home at Syracuse, New York.[18] This difference in the maximum OH production rates, with the same background HONO levels of a few ppbs, can be ascribed to the higher J(HONO) = 1.5×10^{-4} s^{-1} measured in direct sunlight in the indoor environment in Guangzhou compared to J(HONO) = 7.2×10^{-5} s^{-1} measured in a sunlit area in the home in Syracuse, New York.[18]

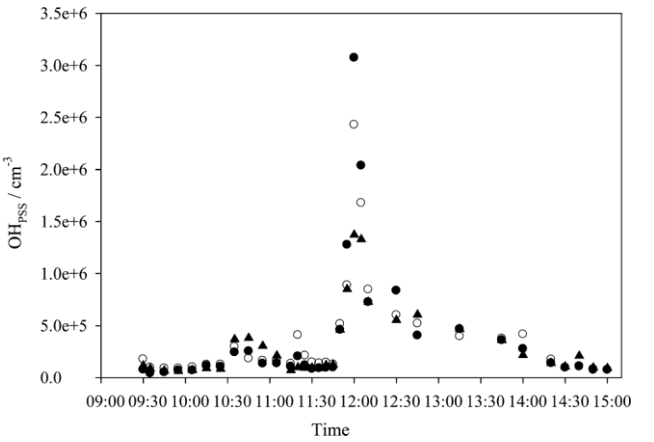

Fig. 4 The estimated OH_{PSS} concentrations in the room located on the campus of JNU, Guangzhou, China, (**B**) in the absence of human activity, (▲) in the presence of cooking (10:15–10:30), and (**C**) in the presence of cooking (11:45–12:00).

Conclusions

The observed results from this study show that under "high NO_x" conditions (NO_x higher than a few ppb), OH could peak indoors at 3.1×10^6 cm^{-3} for certain periods of the day when sunlight directly irradiates the room. This modelled OH value is similar to the directly measured peak OH values of 1.8×10^6 cm^{-3} under "high NO_x" conditions in the classroom in Marseille.[17]

This shows that in sunlit areas of a kitchen or a bedroom, the OH concentrations would reach identical peak values, which in turn are similar to the outdoor OH values. However, this is only valid if radical propagation by VOC oxidation is fast.[62,67] These results demonstrate that under "high NO_x" conditions, the NO_x and HONO chemistry would be pretty much similar, independent of the geographic location of the indoor environment. In addition, the similarity of the measured spectral irradiances in this indoor environment in China with some previous measurements in the EU[17,29] and US[31] is an important outcome of this study with respect to future modelling studies of indoor air photochemistry. The similar J(HONO) values is of particular importance regarding the modelling of OH radical chemistry. An important conclusion drawn from this work is that OH concentrations are very similar in the absence of human activity and in the presence of cooking. That is because both case scenarios are considered as "high NO_x" conditions, which is always the case in residences. The sub ppb levels of NO_x can only be detected in some administration buildings that are located far away from intense traffic and other combustion sources.

However, the combination of direct sunlight in the room and various combustion sources (candle, gas stove)[18,73] can lead to different OH concentrations depending on the orientation of the room, as well as the thickness and the nature of the glass windows. For this reason, further measurements of OH radical concentrations constrained with the MCM model, including the transport of species from indoor to outdoor and *vice versa*, are needed in order to obtain a clearer picture of indoor oxidation capacity in the presence of high NO_x levels generated by various combustion processes (candle, gas range, gas plate, gas stove).

OH chemistry can induce the photochemical transformation of VOCs into highly oxidized organic molecules (HOMs)[74] and secondary organic aerosols (SOA) in various indoor environments and potentially affect human health.[3] The OH radicals are expected to be crucial not only for secondary organic aerosol growth but also to new particle formation.[75] Therefore, a comprehensive understanding of OH production under "high NO_x" levels as well as HOMs/SOA on an hour-to-hour and season-to-season basis will be essential to developing more accurate models describing the gas-phase chemistry of indoor environments.

Conflicts of interest

The authors declare no competing financial interests.

Acknowledgements

This work was supported by National Natural Science Foundation of China (No. 41773131). We are grateful to "Hexin Analytical Instrument Co., Ltd., China" for their generous offer to use the SPIMS 3000 during the campaign measurements.

References

1 C. J. Weschler and N. Carslaw, Indoor Chemistry, *Environ. Sci. Technol.*, 2018, 52(5), 2419–2428.

2 S. Gligorovski and J. P. D. Abbatt, An indoor chemical cocktail, *Science*, 2018, 359(6376), 632–633.

3 S. Gligorovski, X. Li and H. Herrmann, Indoor (Photo) chemistry in China and Resulting Health Effects, *Environ. Sci. Technol.*, 2018, 52, 10909–10910.

4 W. S. Beckett, M. B. Russi, A. D. Haber, R. M. Rivkin, J. R. Sullivan, Z. Tameroglu, V. Mohsenin and B. P. Leaderer, Effect of Nitrous Acid on Lung Function in Asthmatics: A Chamber Study, *Environ. Health Perspect.*, 1995, 103, 372–375.

5 T. R. Rasmussen, M. Brauer and S. Kjaergaard, Effects of nitrous acid exposure on human mucous membranes, *Am. J. Respir. Crit. Care Med.*, 1995, 151, 1504–1511.

6 P. L. Hanst, Air pollution measurement by fourier transform spectroscopy, *Appl. Opt.*, 1978, 17, 1360–1366.

7 J. N. Pitts Jr, D. Grosjean, K. Van Cauwenberghe, J. P. Schmid and D. R. Fitz, Photooxidation of aliphatic amines under simulated atmospheric conditions: Formation of nitrosamines, nitramines, amides and photochemical oxidant, *Environ. Sci. Technol.*, 1978, 12, 946–953.

8 M. Sleiman, L. A. Gundel, J. F. Pankow, P. Jacob, B. C. Singer and H. Destaillats, Formation of carcinogens indoors by surface-mediated reactions of nicotine with nitrous acid, leading to potential thirdhand smoke hazards, *Proc. Natl. Acad. Sci. U. S. A.*, 2010, 107(15), 6576–6581.

9 Z. Večeřa and P. K. Dasgupta, Indoor Nitrous Acid Levels. Production of Nitrous Acid from Open-Flame Sources, *Int. J. Environ. Anal. Chem.*, 1994, 56, 311–316.

10 A. Febo and C. Perrino, Prediction and experimental evidence for high air concentration of nitrous acid in indoor environments, *Atmos. Environ.*, 1991, 25, 1055–1061.

11 N. A. Katsanos, F. De Santis, A. Cordoba, F. Roubani-Kalantzopoulou and D. Pasella, Corrosive effects from the deposition of gaseous pollutants on surfaces of cultural and artistic value inside museums, *J. Hazard. Mater.*, 1999, 64(1), 21–36.

12 J. D. Spengler, M. Brauer, J. M. Samet and W. E. Lambert, Nitrous acid in Albuquerque, New Mexico, homes, *Environ. Sci. Technol.*, 1993, 27, 841–845.

13 P. K. Simon and P. K. Dasgupta, Continuous automated measurement of gaseous nitrous and nitric acids and particulate nitrite and nitrate, *Environ. Sci. Technol.*, 1995, 29, 1534–1541.

14 K. Lee, J. Xue, A. S. Geyh, H. Özkaynak, B. P. Leaderer, C. J. Weschler and J. D. Spengler, Nitrous Acid, nitrogen dioxide, and ozone concentrations in residential environments, *Environ. Health Perspect.*, 2002, 110, 145–149.

15 M. I. Khoder, Nitrous acid concentrations in homes and offices in residential areas in Greater Cairo, *J. Environ. Monit.*, 2002, 4, 573–578.

16 S. S. Park and S. Y. Cho, Performance Evaluation of an *In Situ* Nitrous Acid Measurement System and Continuous Measurement of Nitrous Acid in an Indoor Environment, *J. Air Waste Manage. Assoc.*, 2012, 60, 1434–1442.

17 E. Gómez Alvarez, D. Amedro, C. Affo, S. Gligorovski, C. Schoemacker, C. Fittschen, J. F. Doussin and H. Wortham, Unexpectedly high indoor hydroxyl radical concentrations associated with nitrous acid, *Proc. Natl. Acad. Sci. U. S. A.*, 2013, 110(33), 13294–13299.

18 S. Zhou, C. J. Young, T. C. VandenBoer, S. F. Kowal and T. F. Kahan, Time-Resolved Measurements of Nitric Oxide, Nitrogen Dioxide, and Nitrous Acid in an Occupied New York Home, *Environ. Sci. Technol.*, 2018, 52(15), 8355–8364.

19 F. Sakamaki, S. Hatakeyama and H. Akimoto, Formation of nitrous acid and nitric oxide in the heterogeneous dark reaction of nitrogen dioxide and water vapour in a smog chamber, *Int. J. Chem. Kinet.*, 1983, 15, 1013–1029.

20 K. A. Ramazan, D. Syomin and B. J. Finlayson-Pitts, The photochemical production of HONO during the heterogeneous hydrolysis of NO_2, *Phys. Chem. Chem. Phys.*, 2004, 6(14), 3836–3843.

21 K. A. Ramazan, L. M. Wingen, Y. Miller, G. M. Chaban, R. B. Gerber, S. S. Xantheas and B. J. Finlayson-Pitts, New Experimental and Theoretical Approach to the Heterogeneous Hydrolysis of NO_2: Key Role of Molecular Nitric Acid and Its Complexes, *J. Phys. Chem. A*, 2006, 110(21), 6886–6897.

22 B. J. Finlayson-Pitts, L. M. Wingen, A. L. Sumner, D. Syomin and K. A. Ramazan, The heterogeneous hydrolysis of NO_2 in laboratory systems and in outdoor and indoor atmospheres: An integrated mechanism, *Phys. Chem. Chem. Phys.*, 2003, 5, 223–242.

23 E. Gomez Alvarez, M. Sörgel, S. Gligorovski, S. Bassil, V. Bartolomei, B. Coulomb, C. Zetzsch and H. Wortham, Light-induced nitrous acid (HONO) production from NO_2 heterogeneous reactions on household chemicals, *Atmos. Environ.*, 2014, 95, 391–399.

24 V. Bartolomei, M. Sorgel, S. Gligorovski, E. Gomez Alvarez, A. Gandolfo, R. Strekowski, E. Quivet, A. Held, C. Zetzsch and H. Wortham, Formation of indoor nitrous acid (HONO) by light-induced NO_2 heterogeneous reactions with white wall paint, *Environ. Sci. Pollut. Res.*, 2014, 21, 9259–9269.

25 A. Gandolfo, V. Bartolomei, E. Gomez Alvarez, S. Tlili, S. Gligorovski, J. Kleffmann and H. Wortham, The effectiveness of indoor photocatalytic paints on NO_x and HONO levels, *Appl. Catal., B*, 2015, 166–167, 84–90.

26 A. Gandolfo, L. Rouyer, H. Wortham and S. Gligorovski, The influence of wall temperature on NO_2 removal and HONO levels released by indoor photocatalytic paints, *Appl. Catal., B*, 2017, 209, 429–436.

27 S. Gligorovski, Nitrous acid (HONO): An emerging indoor pollutant, *J. Photochem. Photobiol., A*, 2016, 314, 1–5.

28 X. Li, S. Gligorovski and H. Herrmann, Underestimated contribution of HONO to indoor OH radicals: an emerging concern, *Sci. Bull.*, 2018, 63, 1383–1384.

29 A. Gandolfo, V. Gligorovski, V. Bartolomei, S. Tlili, E. Gomez Alvarez, H. Wortham, J. Kleffmann and S. Gligorovski, Spectrally resolved actinic flux and photolysis frequency of key species within indoor environment, *Build. Environ.*, 2016, 109, 50–57.

30 M. Blocquet, F. Guo, M. Mendez, M. Ward, S. Coudert, S. Batut, C. Hecquet, N. Blond, C. Fittschen and C. Schoemaecker, Impact of the spectral and spatial properties of natural light on indoor gas-phase chemistry: Experimental and modeling study, *Indoor Air*, 2018, 28, 426–440.

31 S. F. Kowal, S. R. Allen and T. F. Kahan, Wavelength-Resolved Photon Fluxes of Indoor Light Sources: Implications for HO_x Production, *Environ. Sci. Technol.*, 2017, 51(18), 10423–10430.

32 J. Kleffmann, Comment on "Wavelength-Resolved Photon Fluxes of Indoor Light Sources: Tara F. Kahan, Implications for HO_x Production", *Environ. Sci. Technol.*, 2018, 52, 11964–11965.

33 T. F. Kahan, Response to Comment on "Wavelength-Resolved Photon Fluxes of Indoor Light Sources: Implications for HO_x Production", *Environ. Sci. Technol.*, 2018, 52, 11966–11967.

34 H. Schwartz-Narbonne, S. Jones, D. Helen and J. Donaldson, Indoor Lighting Releases Gas Phase Nitrogen Oxides From Indoor Painted Surfaces, *Environ. Sci. Technol. Lett.*, 2019, 6(2), 92–97.

35 N. Carslaw, A new detailed chemical model for indoor air pollution, *Atmos. Environ.*, 2007, 41, 1164–1179.

36 S. Gligorovski, R. Strekowski, S. Barbati and D. Vione, The environmental implications of hydroxyl radical (OH), *Chem. Rev.*, 2015, 115(24), 13051–13092.

37 S. Gligorovski and C. J. Weschler, The oxidative capacity of indoor atmospheres, *Environ. Sci. Technol.*, 2013, 47, 13905–13906.

38 H. Schwartz-Narbonne, C. Wang, S. Zhou, J. P. Abbatt and J. Faust, Heterogeneous chlorination of squalene and oleic acid, *Environ. Sci. Technol.*, 2019, 53(3), 1217–1224.

39 C. K. Borrowman, S. Zhou, T. E. Burrow and J. P. Abbatt, Formation of environmentally persistent free radicals from the heterogeneous reaction of ozone and polycyclic aromatic compounds, *Phys. Chem. Chem. Phys.*, 2016, 18, 205–212.

40 N. Borduas, J. P. D. Abbatt, J. G. Murphy, S. So and G. da Silva, Gas-Phase Mechanisms of the Reactions of Reduced Organic Nitrogen Compounds with OH Radicals, *Environ. Sci. Technol.*, 2016, 50, 11723–11734.

41 S. Zhou, M. W. Forbes, Y. Katrib and J. P. D. Abbatt, Rapid Oxidation of Skin Oil by Ozone, *Environ. Sci. Technol. Lett.*, 2016, 3, 170–174.

42 N. Carslaw, L. Fletcher, D. Heard, T. Ingham and H. Walker, Significant OH production under surface cleaning and air cleaning conditions: impact on indoor air quality, *Indoor Air*, 2017, 27(6), 1091–1100.

43 J. N. Pitts Jr, T. J. Wallington, H. W. Biermann and A. M. Winer, Identification and Measurement of Nitrous

Acid in an Indoor Environment, *Atmos. Environ.*, 1985, 19, 763–767.

44 S. S. Park, J. H. Hong, J. H. Lee, Y. J. Kim, S. Y. Cho and S. J. Kim, Investigation of nitrous acid concentration in an indoor environment using an *in situ* monitoring system, *Atmos. Environ.*, 2008, 42(27), 6586–6596.

45 J. Stutz, H.-J. Oh, S. I. Whitlow, C. Anderson, J. E. Dibb, J. H. Flynn, B. Rappenglück and B. Lefer, Simultaneous DOAS and mist-chamber IC measurements of HONO in Houston, TX, *Atmos. Environ.*, 2010, 44, 4090–4098.

46 J. P. Pinto, J. Dibb, B. H. Lee, B. Rappenglück, E. C. Wood, M. Levy, R.-Y. Zhang, B. Lefer, X.-R. Ren, J. Stutz, C. Tsai, L. Ackermann, J. Golovko, S. C. Herndon, M. Oakes, Q.-Y. Meng, J. W. Munger, M. Zahniser and J. Zheng, Intercomparison of field measurements of nitrous acid (HONO) during the SHARP campaign, *J. Geophys. Res.: Atmos.*, 2014, 119, 5583–5601.

47 C. W. Spicer, I. H. Billick and Y. Yanagisawa, Nitrous Acid Interference with Passive NO_2 Measurement Methods and the Impact on Indoor NO_2 Data, *Indoor Air*, 2001, 11, 156–161.

48 J. Heland, J. Kleff mann, R. Kurtenbach and P. Wiesen, A New Instrument To Measure Gaseous Nitrous Acid (HONO) in the Atmosphere, *Environ. Sci. Technol.*, 2001, 35, 3207–3212.

49 J. Kleff mann, J. Heland, R. Kurtenbach, J. C. Lorzer and P. Wiesen, A New Instrument (LOPAP) for the Detection of Nitrous Acid (HONO), *Environ. Sci. Technol.*, 2002, 9(4), 48–54.

50 G. Villena, I. Bejan, R. Kurtenbach, P. Wiesen and J. Kleff mann, Interferences of commercial NO_2 instruments in the urban atmosphere and in a smog chamber, *Atmos. Meas. Tech.*, 2012, 5, 149–159.

51 W. Gao, G. B. Tan, Y. Hong, M. Li, H. Q. Nian, C. J. Guo, Z. X. Huang, Z. Fu, J. G. Dong, X. Xu, P. Cheng and Z. Zhou, Development of portable single photon ionization time-of-flight mass spectrometer combined with membrane inlet, *Int. J. Mass Spectrom.*, 2013, 334, 8–12.

52 L. A. Wallace, S. J. Emmerich and C. Howard-Reed, Continuous measurements of air change rates in an occupied house for 1 year: The eff ect of temperature, wind, fans, and windows, *J. Exposure Anal. Environ. Epidemiol.*, 2002, 12, 296–306.

53 D. B. Collins, R. F. Hems, S. Zhou, C. Wang, E. Grignon, M. Alavy, J. A. Siegel and J. P. D. Abbatt, Evidence for Gas-Surface Equilibrium Control of Indoor Nitrous Acid, *Environ. Sci. Technol.*, 2018, 52, 12419–12427.

54 S. Zhou, C. J. Young, T. C. VandenBoer and T. F. Kahan, Role of location, season, occupant activity, and chemistry in indoor ozone and nitrogen oxide mixing ratios, *Environ. Sci.: Processes Impacts*, 2019, DOI: 10.1039/c9em00129h.

55 S. Madronich, Intercomparison of NO_2 photodissociation and UV radiometer measurements, *Atmos. Environ.*, 1987, 21, 569–578.

56 B. J. Finlayson-Pitts and J. N. Pitts Jr, *Chemistry of the Upper and Lower atmosphere. Theory, Experiments, and Application*, Academic Press, San Diego, 2000.

57 W. B. DeMore, S. P. Sander, D. M. Golden, R. F. Hampson, M. J. Kurylo, C. J. Howard, A. R. Ravishankara, C. E. Kolb and M. J. Molina, Chemical Kinetics and Photochemical Data for Use in Stratospheric Modeling in *JPL Publication 97-4*, Jet Propulsion Laboratory, Pasadena, CA, 1997.

58 J. Stutz, E. S. Kim, U. Platt, P. Bruno, C. Perrino and A. Febo, A UV-visible absorption cross sections of nitrous acid, *J. Geophys. Res.: Atmos.*, 2000, 105(D11), 14585–14592.

59 R. A. Cox and R. G. Derwent, The Ultraviolet Absorption Spectrum of Gaseous Nitrous Acid, *J. Photochem.*, 1976/77, 6, 23–34.

60 K. D. Lu, F. Rohrer, F. Holland, H. Fuchs, B. Bohn, T. Brauers, C. C. Chang, R. Häseler, M. Hu, K. Kita, Y. Kondo, X. Li, S. R. Lou, S. Nehr, M. Shao, L. M. Zeng, A. Wahner, Y. H. Zhang and A. Hofzumahaus, Observation and modelling of OH and HO_2 concentrations in the Pearl River Delta 2006: a missing OH source in a VOC rich atmosphere, *Atmos. Chem. Phys.*, 2012, 12, 1541–1569.

61 B. Alicke, A. Geyer, A. Hofzumahaus, F. Holland, S. Konrad, H. W. Pätz, J. Schäfer, J. Stutz, A. Volz-Thomas and U. Platt, OH formation by HONO photolysis during the BERLIOZ experiment, *J. Geophys. Res.: Atmos.*, 2003, 108, 8247, DOI: 10.1029/2001jd000579.

62 Y. F. Elshorbany, R. Kurtenbach, P. Wiesen, E. Lissi, M. Rubio, G. Villena, E. Gramsch, A. R. Rickard, M. J. Pilling and J. Kleff mann, Oxidation capacity of the city air of Santiago, Chile, *Atmos. Chem. Phys.*, 2009, 9, 2257–2273.

63 C. Topaloglou, S. Kazadzis, A. F. Bais, M. Blumthaler, B. Schallhart and D. Balis, NO_2 and HCHO photolysis frequencies from irradiance measurements in Thessaloniki, Greece, *Atmos. Chem. Phys.*, 2005, 5, 1645–1653.

64 B. P. Leaderer, L. Naeher, T. Jankun, K. Balenger, T. R. Holford, C. Toth, J. Sullivan, J. M. Wolfson and P. Koutrakis, Indoor, outdoor, and regional summer and winter concentrations of PM10, PM2.5, SO_4^{2-}, H^+, NH_4^+, NO_3^-, NH_3, and nitrous acid in homes with and without kerosene space heaters, *Environ. Health Perspect.*, 1999, 107(3), 223–231.

65 J. N. Pitts Jr, E. Sanhueza, R. Atkinson, W. P. L. Carter, A. M. Winer, G. W. Harris and C. N. Plum, An Investigation of the Dark Formation of Nitrous Acid in Environmental Chambers, *Int. J. Chem. Kinet.*, 1984, 16, 919–939.

66 A. Wisthaler and C. J. Weschler, Reactions of ozone with human skin lipids: Sources of carbonyls, dicarbonyls, and hydroxycarbonyls in indoor air, *Proc. Natl. Acad. Sci. U. S. A.*, 2010, 107(15), 6568–6575.

67 Y. F. Elshorbany, J. Kleff mann, R. Kurtenbach, E. Lissi, M. Rubio, G. Villena, E. Gramsch, A. R. Rickard, M. J. Pilling and P. Wiesen, Seasonal dependence of the oxidation capacity of the city of Santiago de Chile, *Atmos. Environ.*, 2010, 44, 5383–5394.

68 Y. Elshorbany, I. Barnes, K. H. Becker, J. Kleff mann and P. Wiesen, Sources and Cycling of Tropospheric Hydroxyl Radicals – An Overview, *Z. Phys. Chem.*, 2010, 224, 967–987.

69 X. Ren, W. H. Brune, J. Mao, M. J. Mitchell, R. L. Lesher, J. B. Simpas, A. R. Metcalf, J. J. Schwab, C. Cai, Y. Li, K. L. Demerjian, H. D. Felton, G. Boynton, A. Adams, J. Perry, Y. He, X. Zhou and J. Hou, Behavior of OH and HO_2 in the Winter Atmosphere in New York City, *Atmos. Environ.*, 2006, 40(Suppl. 2), 252–263.

70 Y. Kanaya, R. Cao, H. Akimoto, M. Fukoda, Y. Komazaki, Y. Yokouchi, M. Koike, H. Tanimoto, N. Takegawa and Y. Konodo, Urban photochemistry in central Tokyo: 1. Observed and modelled OH and HO_2 radical concentrations during the winter and summer of 2004, *J. Geophys. Res.: Atmos.*, 2007, 112, D21312, DOI: 10.1029/2007jd008670.

71 K. M. Emmerson, N. Carslaw and M. J. Pilling, Urban Atmospheric Chemistry during the PUMA Campaign. 2: Radical budgets for OH, HO_2 and RO_2, *J. Atmos. Chem.*, 2005, 52, 165–183.

72 N. Carslaw, A new detailed chemical model for indoor air pollution, *Atmos. Environ.*, 2007, 41, 1164–1179.

73 V. Bartolomei, E. Gomez Alvarez, J. Wittmer, S. Tlili, R. Strekowski, B. Temime-Roussel, E. Quivet, H. Wortham, C. Zetzsch, J. Kleff mann and S. Gligorovski, Combustion Processes as a Source of High Levels of Indoor Hydroxyl Radicals through the Photolysis of Nitrous Acid, *Environ. Sci. Technol.*, 2015, 49(11), 6599–6607.

74 T. Berndt, S. Richters, T. Jokinen, N. Hyttinen, T. Kurten, R. V. Otkjær, H. G. Kjaergaard, F. Stratmann, H. Herrmann, M. Sipila, M. Kulmala and M. Ehn, Hydroxyl radical-induced formation of highly oxidized organic compounds, *Nat. Commun.*, 2016, 7, 13677–13684.

75 T. Jokinen, M. Sipil, S. Richters, V.-M. Kerminen, P. Paasonen, F. Stratmann, D. Worsnop, M. Kulmala, M. Ehn, H. Herrmann and T. Berndt, Rapid autoxidation forms highly oxidized RO_2 radicals in the atmosphere, *Angew. Chem., Int. Ed.*, 2014, 53, 14596–14600.